



QUASI-STATIC CYCLIC TESTS ON U-SHAPED RC WALLS: TEST DESIGN AND PRELIMINARY RESULTS

Katrin BEYER¹, Alessandro DAZIO² and M.J. Nigel PRIESTLEY³

SUMMARY

U-shaped or channel-shaped walls are frequently used as lateral strength providing members in RC buildings since their form does not only provide strength and stiffness in any horizontal direction but is also well suited to accommodate lift shafts or stair cases. Although U-shaped walls are very popular in practice experimental results on their behaviour under seismic loading are very sparse and codes do not provide detailed guidelines for their design when a ductile behaviour is aimed for. In this context a test program was developed comprising two U-shaped walls at 1:2 scale with the aim to contribute to the understanding of the behaviour of ductile U-shaped walls under seismic loading. The main difference between the two test units is the wall thickness. In this paper the design of the test units is briefly presented. The paper also includes a discussion on the main decisions regarding the test setup. These comprise the design of the load stub which controls warping of the top section and the displacement loading history in bending and torsion. Finally, preliminary results from the first wall are briefly presented.

1. INTRODUCTION

Over the last decades the seismic behaviour of reinforced concrete (RC) walls with a rectangular cross section has been the subject of extended research. Several test series on such walls have been completed, most of these were quasi-static cyclic tests (e.g. Vallenias et al. [1979], Oesterle et al. [1980], Paulay et al. [1982], Elnashai et al. [1990], Dazio et al. [1999], Salonikis et al. [1999]), others were dynamic tests (e.g. Lestuzzi et al. [1999], ECOEST2/ICONS [2001]). As a direct consequence of these experiments the behaviour of rectangular walls under seismic excitation is nowadays fairly well understood and the key parameters yielding a reliable and desirable behaviour of such walls during an earthquake are identified. The knowledge on the key parameters was in turn translated into code provisions giving detailed guidelines to the designer.

Despite their popularity in real designs only very few experiments on U-shaped walls under seismic loading have been conducted. The largest test series to our knowledge has been jointly conducted at the research laboratories in Ispra and Saclay (Ile et al. [2002], Ile and Reynouard [2005]). Within the scope of this test series a single wall configuration was subjected to different types of loading. The U-shaped wall was designed for medium ductility level according to Eurocode 8 [2003]. The test series which is described here aims to complement these experiments by carrying out quasi-static cyclic tests on U-shaped walls with different cross sections to the one tested in Ispra and Saclay. In addition, the walls are designed for high ductility instead of medium ductility.

¹ Rose School, European School for Advanced Studies in Reduction of Seismic Risk, c/o EUCENTRE, Via Ferrata 1, 27100 Pavia, Italy
Email : kbeyer@roseschool.it

² Institute of Structural Engineering (IBK), ETH Zürich, Wolfgang-Pauli-Strasse 15, 8093 Zürich, Switzerland
Email: dazio@ibk.baug.ethz.ch

³ Rose School, European School for Advanced Studies in Reduction of Seismic Risk, c/o EUCENTRE, Via Ferrata 1, 27100 Pavia, Italy
Email : nigelpriestley@xtra.co.nz

The aim of the test series is to gain experimental evidence for stiffness, strength and displacement capacity of U-shaped walls when loaded in different directions. In addition, the rotational stiffness of U-shaped walls is also assessed. The experiments will be complemented by analytical investigations. The final objective of the research program is to make a contribution to more detailed design guidelines for ductile U-shaped walls.

In the following sections a brief summary of the development of the test units on the basis of a reference building is described (Section 2), the predictions regarding the flexural and shear behaviour of test unit A is summarised (Section 3), the details of the experimental setup and the loading history are outlined (Section 4) and preliminary results of the first test unit are presented (Section 5).

2. DEVELOPMENT OF TEST UNITS

2.1 Reference Building

The starting point for designing the test units was a fictitious 6-storey reference building for which the lateral force resisting elements comprised one U-shaped wall and a bi-directional moment resisting frame system. The dimensions of the U-shaped wall were those typical of a shaft housing an 8-person lift. An isometric and a plan view of the reference building are shown in Figure 1. In the plan view also shown is the assumed tributary area for the U-shaped wall based on which the axial force on the U-shaped wall was determined. Although the centre of the tributary area does not coincide with the centre of the wall, this eccentricity was not accounted for in the experiments and the axial load was applied at the gravity centre of the cross sections. The seismic hazard to the building was defined in terms of the elastic design spectrum of Type 1 given in Eurocode 8 [2003] with a peak ground acceleration of $0.3g$, an importance factor of unity and for a soil class B.

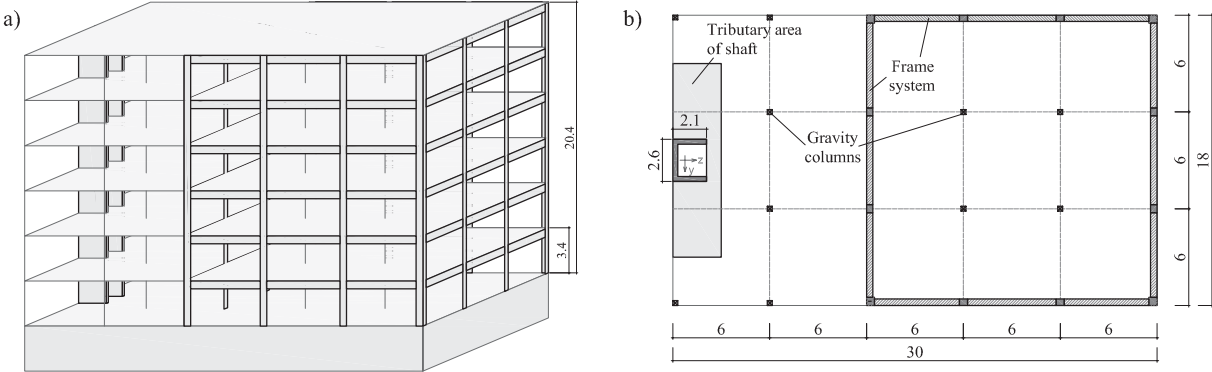


Figure 1: 6-storey reference building: Isometric (a) and plan view (b), all dimensions in m

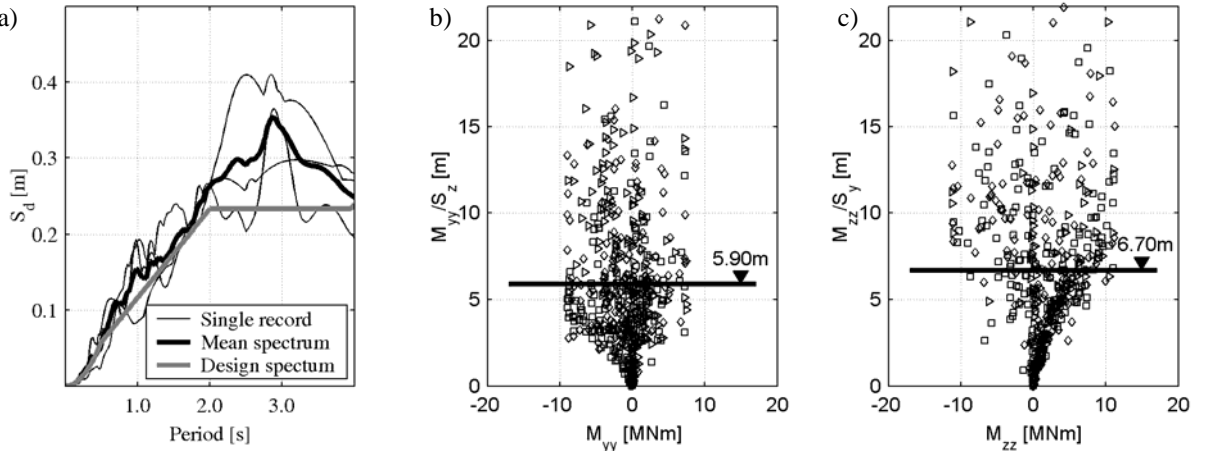


Figure 2: 5% damped elastic design displacement spectrum and spectra of real records used for the analysis of the reference building (a) and ratios of base moment to base shear of the U-shaped wall plotted against the base moment for the two principal directions (b+c)

When carrying out quasi-static cyclic tests the shear span, i.e. the ratio of moment to shear force, is fixed during the experiment since the height of the actuator with respect to the base section of the wall is fixed. Non-linear time history analyses were carried out to locate the moment/shear ratios at the base and to check the magnitude of the rotations of the building. The lowest base moment/ base shear ratios for which the full moment capacities were attained were selected as shear spans in the two principal directions for the quasi-static tests (Figure 2b and Figure 2c). Practical considerations regarding the test set-up required slight adaptations to the effective heights. The final shear spans of the full-scale wall were 5.9m in the direction parallel to the flanges and 6.7m in the direction parallel to the web.

2.2 Sections of Test Units

The moment and shear demands on the prototype U-shaped wall of the reference building were determined according to Eurocode 8 [2003] combining the demand due to excitation in x - and y -direction with the “30%-rule”. Based on the section forces at the wall base two cross sections of test units at 1:2 scale were developed. By also scaling the maximum aggregate size from 32mm to 16mm it was attempted to keep scaling effects small. The test program comprises two different test units A and B. The wall thickness was chosen as the main parameter which varies between the two units since it is considered a key parameter regarding the overall behaviour of the wall. More specifically, it affects - together with the concrete strength - the shear capacity of the wall and the depth of the compression zone and hence the strain demand on the concrete. The latter is expected to be particular of concern when loading is applied in diagonal direction (Section 4.2). The cross sections of test unit A and B are shown in Figure 3. Also shown is the cross section of the U-shaped wall which was tested under quasi-static loading in Ispra. The main parameters of the three walls are summarised in Table 1. The comparison shows that test units A and B complement the Ispra-experiment well regarding slenderness ratios, reinforcement ratios and detailing of the boundary elements.

Table 1: Key dimensions and ratios of test units A and B and of wall tested at Ispra

	Test Unit A	Test Unit B	Ispra
Scale	1:2	1:2	1:1
Wall thickness	150mm	100mm	250mm
Shear span h	3.35m/2.95m	3.35m/2.95m	3.90m
Slenderness h/l_w	2.58/2.81	2.58/2.81	2.60/3.12
Total reinforcement ratio ρ_{tot}	0.71%	0.95%	0.56%
Axial load (axial load ratio $N/A_g f_c'$)	780kN (0.04)	780kN (0.04)	2000kN (0.10)

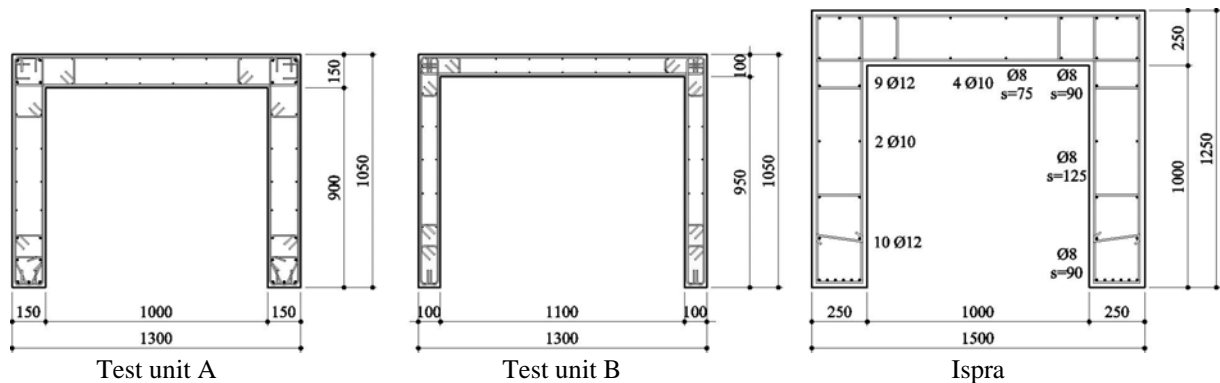


Figure 3: Cross sections of test units A and B and of wall tested at Ispra (all dimensions in mm)

Since the test units are also subjected to torsional loading the constraints imposed by the load stub on warping of the wall were considered. If the load stub is constructed as a thick top plate warping of the wall is almost completely restraint. To illustrate the effect of respectively restraining or not restraining warping, Figure 4a shows the variation of rotation with height of a U-shaped wall with the dimensions of test unit A when subjected to an arbitrary torsional moment of $T=100kNm$ at $h=2.95m$ (analytical closed-form solution for a cantilever wall [Petersen, 1997]). The results show that restraining warping stiffens the wall significantly. It also changes the way the flanges carry the load since the top slab introduces an in-plane force-couple at the top of each flange; the

entity of the two counter-rotating force-couples is also called bimoment [Heidebrecht and Stafford Smith, 1973]. If no top slab is provided the top edge of the flanges is stress-free and the flanges carry the shear due to the torsional moment as cantilever walls in bending. In a real building floor slabs will provide partial restraint to warping and introduce bimoments into the wall at the storey levels. Heidebrecht and Stafford Smith [1973] developed an approximative approach to account for the warping restraint provided by floor slabs. To include this effect in the analytical solutions the stiffness of one slab is smeared over a storey height. Figure 4b shows the variation of rotation with height of a U-shaped wall of the reference building for four different cases: First, (cases 1 and 2) the U-shaped wall of the reference building is considered including the stiffening effect of the floor slabs. The system is analysed for two types of loading for which closed-form solutions are available, i.e. end moment ($T=800kNm$) and a constant distributed moment ($m_T=800kNm/20.4m=39.2kNm/m'$). Note that a moment of $800kNm$ on the full-scale section corresponds to a moment of $100kNm$ on the half scale model since moments scale with the third power of the scaling factor. The actual shape of the torsional load on the U-shaped wall during an earthquake will vary; the two analysed cases are expected to bound the expected shapes of torsional loads. Second, (cases 3 and 4) the U-shaped wall with the height as it will be modelled in the experiment is considered (i.e. twice the height of the test units). In the experiment, the wall can only be subjected to end moments. The system was analysed for the two different end condition, restrained and unrestrained warping. Comparison to the rotation profiles of the full-height wall cases show that the wall where the top edge is unrestrained matches the full-height wall cases best regarding shape of the rotation profile and the torsional stiffness. In the construction of the test units the top edge of the wall was strengthened by a “collar” as shown in Figure 7b which provides some restraint to warping but significantly less than a solid top plate which would prohibit warping almost completely. Some strengthening of the top edge of the wall was required for applying the actuator forces without causing large local deformations. The walls tested at Ispra [Ile and Reynouard, 2005] were restrained by a solid top plate. However, the walls were not subjected to rotations but to translations only. The influence of the boundary condition on the behaviour in flexure is still under investigation. The analytical calculations presented here are only one part of a larger set of analyses performed to assess the behaviour of U-shaped walls under torsion. Linear elastic models were included since only fairly small rotations will be applied in the experiment.

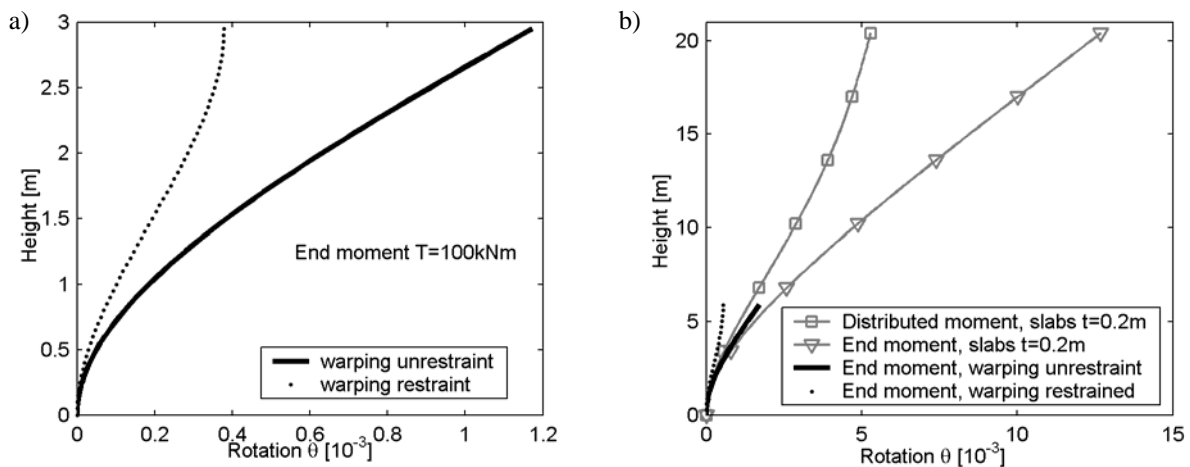


Figure 4: Rotation of an elastic, homogenous U-shaped cantilever wall with the cross section dimensions of test unit A under an end torsional moment of $T=100kNm$ for restrained and unrestrained warping at the top (a); Comparison of rotational shapes when subjected to torsional moments of $T=800kNm$ of the full-height wall and of the wall with the height modelled in the experiment (b)

2.3 Material Properties

Regarding the concrete it was aimed to model a concrete C30/37 several years of age, since most structures subjected to an earthquake during their life cycle are hit several years after construction has been completed. The characteristic 28d cylinder strength of such a concrete is 30MPa, the mean cylinder strength $f_c'=38MPa$ [Eurocode 2, 2002]. In the experiment a concrete with a mean cylinder strength of 45MPa at the day of testing was strived for. Five years after construction the strength of a typical concrete is about 20% higher than the 28d strength. This increase in strength was accounted for by the margin between 45MPa and 38MPa ($45/38=1.18$). Unfortunately, the recipe for the concrete mixture for test unit A was erroneous and the concrete strength turned

out much higher than intended. The cylinder strength at the day of testing was 74MPa, i.e. 65% higher than aimed for. Test unit B was not yet constructed at the time of writing but a strength of $f_c'=45\text{MPa}$ will be targeted. The design of both test units was carried out under the assumption of $f_c'=45\text{MPa}$.

The reinforcing steel fulfils the Eurocode 8 [2003] requirements for Class C Steel. The mean properties of the D12 and D6 bars used for test unit A are summarised in Table 2.

Table 2: Properties of reinforcement steel used for construction of test unit A

	f_y [MPa]	f_t [MPa]	f_t/f_y [-]	ϵ_u [%]
D12 bars	502	613	1.22	11.9
D6 bars	520	688	1.32	7.7

3. PREDICTION OF THE BEHAVIOUR OF TEST UNIT A

Since the aim of the test program presented in this paper is not to validate existing code provisions but to contribute to the understanding of the behaviour of U-shaped walls under cyclic loading in general, no code was strictly followed during design of the test units. Several codes and research papers were however consulted. The aim was to design U-shaped walls which were expected to behave in a ductile manner while incorporating details which could also be easily realised in engineering practice. Hence, design equations were selected which the authors believed to be most adequate without being unnecessarily conservative. The following paragraphs summarise briefly the predictions for the behaviour of test unit A in flexure and shear.

3.1 Flexural Behaviour

Section analysis of the base sections was carried out using different computer programs. The results presented in Figure 5 were obtained with plastic hinge length method on the basis of moment-curvature relationships obtained with OpenSees [Mazzoni et al., 2005]. Note that since only a section analysis was conducted the predictions do not account for the influence of torsional moments caused by eccentricity of the lateral loads to the shear centre. In the analysis five different directions of loading were considered, i.e.

- parallel to the flanges, flange ends in compression
- parallel to the flanges, web in compression
- parallel to the web
- in diagonal direction, flange end in compression
- in diagonal direction, corner in compression

The diagonal direction had been defined geometrically by joining a corner and the outer angle of the opposite flange end ($\alpha=51^\circ$). The pushover curves show that the displacement capacity is smallest when the wall is loaded in the diagonal direction. This observation is of particular importance since loading in the diagonal direction is often not considered during design, i.e. in most designs of U-shaped walls the most critical loading condition is neglected. Moreover, a large number of section analysis programs do not have the capabilities to analyse U-shaped sections in directions others than parallel to web and flanges. In other programs the U-shaped section is missing in the section library and can only be approximated by a T-section (for loading parallel to the flanges) or an I-section (for loading parallel to the web).

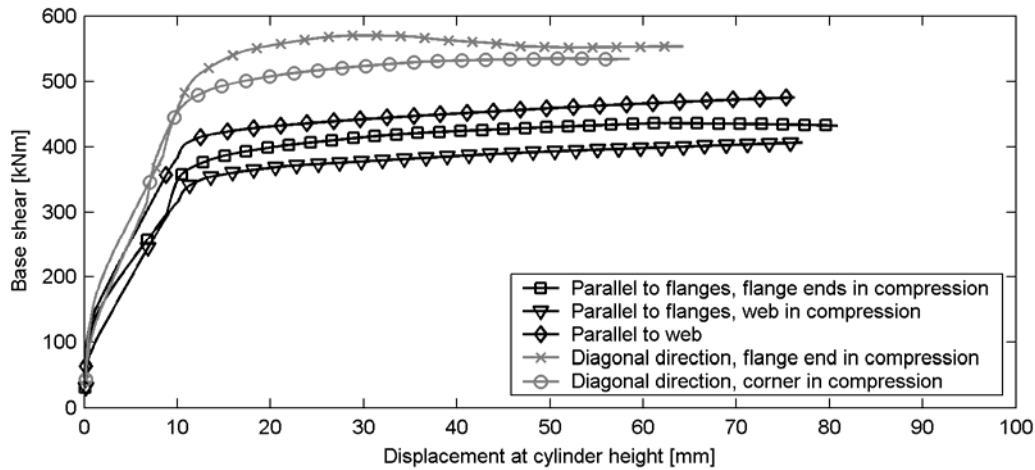


Figure 5: Test unit A: Predicted force-displacement curves for different directions of loading (neglecting tensile strength of concrete)

3.2 Shear Behaviour

Unlike the moment capacity which can be fairly accurately computed if the material properties of steel and concrete are known, estimates for the shear capacity of walls – even of the simple rectangular shape – vary largely between different code provisions or shear models published in the literature. For U-shaped walls additional considerations regarding the distribution of the shear forces on the different wall sections are necessary which harbour more uncertainties for the designer. In the design of the test units the shear force parallel to the web (V_y) was entirely assigned to the web. The shear force parallel to the flanges (V_z) was distributed equally between the two flanges for the cases when the wall was loaded parallel to the symmetry axis. For diagonal loading the shear force was entirely assigned to the flange in compression as suggested in ECOEST2/ICONS [2001]. The web and flanges of the U-shaped walls were then designed as independent rectangular wall sections according to the modified UCSD shear model [Kowalsky and Priestley, 2000]. The approach was complemented by a check on the capacity of the compression strut $V_{Rd,max}$ according to the Swiss code for concrete structures [SIA262, 2004]. On the basis of these equations the shear reinforcement in web and flanges was determined as two layers of D6mm reinforcement every 125mm (see Figure 6a).

Due to their large cross section when compared to rectangular walls the axial load ratio $P/A_g f'_c$ of U-shaped walls tends to be small. Walls with low axial load ratios are particular prone to sliding shear failure. Sliding interfaces are typically cold joints where bond between the two concrete sections is limited, e.g. at the interface between the foundation and the wall. Since sliding was considered a potential failure mode care was taken that the interface between wall and foundation was representative of interfaces in real structures. To achieve this, the wall and foundation were cast in two stages: First, the foundation was cast upright. The surface of the foundation forming the interface with the wall was roughened to an amplitude of about 5mm when the concrete began to become stiff. After a couple of days the wall and foundation were laid horizontally and wall and collar were cast as one entity. Casting the wall upright too was impossible due to height restrictions in the concrete factory. Sliding shear was assessed according to Eurocode 8 [2003] and NZS3101 [2006]. The two code provisions yield very different results. For loading in the direction of the web the sliding shear resistance according to Eurocode 8 is 181kN suggesting sliding shear failure would occur. According to NZS3101 the sliding shear capacity is 2430kN suggesting that this failure mode can be excluded. Moreover, the authors believe that describing the sliding shear phenomena as a friction phenomena at maximum lateral load (as all of the approaches discussed above do) does not account for experimental evidence which has often shown that sliding of a wall subjected to cyclic displacement commonly occurs after load reversal - an observation already made by Paulay and Priestley [1992]. For the sliding shear design of test units A and B a novel approach was developed according to which both walls were prone to sliding shear failure. It was attempted to prevent sliding on the interface between wall and foundation by shear keys (see Figure 6b) which were essentially moulds in the foundation filled with concrete when the wall was cast.

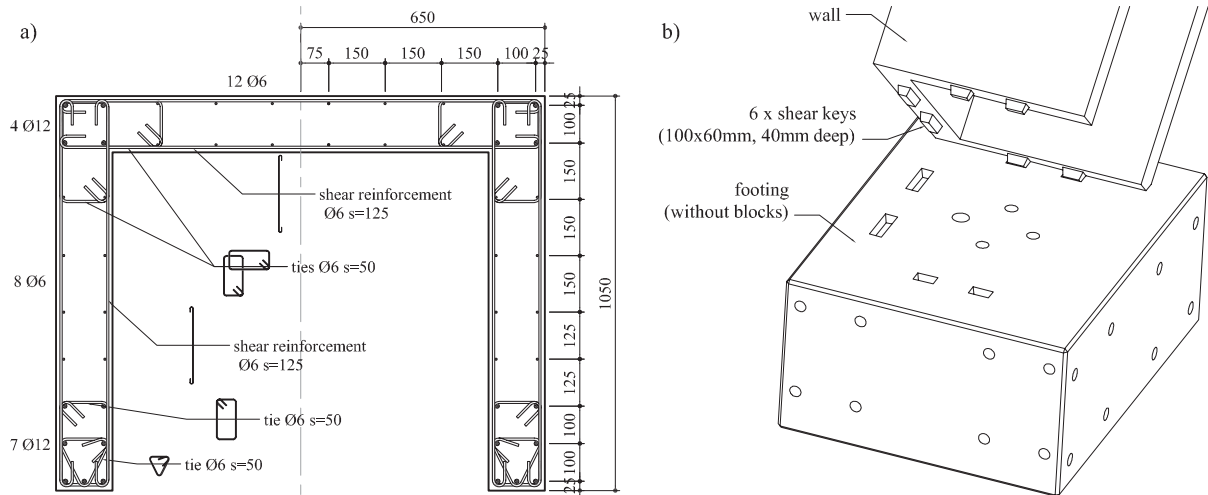


Figure 6: Test unit A: Reinforcement layout (a) and isotropic view of shear keys locking the wall into the foundation (b)

4. QUASI-STATIC CYCLIC TESTING

4.1 Experimental Setup

A photograph of the experimental setup is shown in Figure 7a. It shows that the movement of the wall head is controlled by three servo-hydraulic actuators. With the three actuators it is possible to control displacement and rotation of the wall head. The centre-lines of the actuators are aligned with the centre line of the collar. The actuators parallel to the flanges apply the force 2.95m above the wall base, the actuator parallel to the web is mounted 3.35m above the wall base. The force and displacement capacity of each actuator is 1000kN and 1200mm respectively which is well beyond the requirements for the tests presented here. Each wall is instrumented with 125 channels recording for example global measures (displacements of wall head, forces), curvature, shear deformations, strain of shear reinforcement bars and sliding at wall base. The channels are scanned every 3s. The loading velocity is small to prevent dynamic forces and to allow time for the control of the actuators during the complex loading history (see section 4.2). The velocity is varied between cycles of different ductilities. One load step took approximately 10-20 minutes. The permanent measurements were complemented by manual measurements between the load steps such as crack widths measurements and displacement measurements on a grid of Demag points covering the lower half of the inside faces of web and flanges.

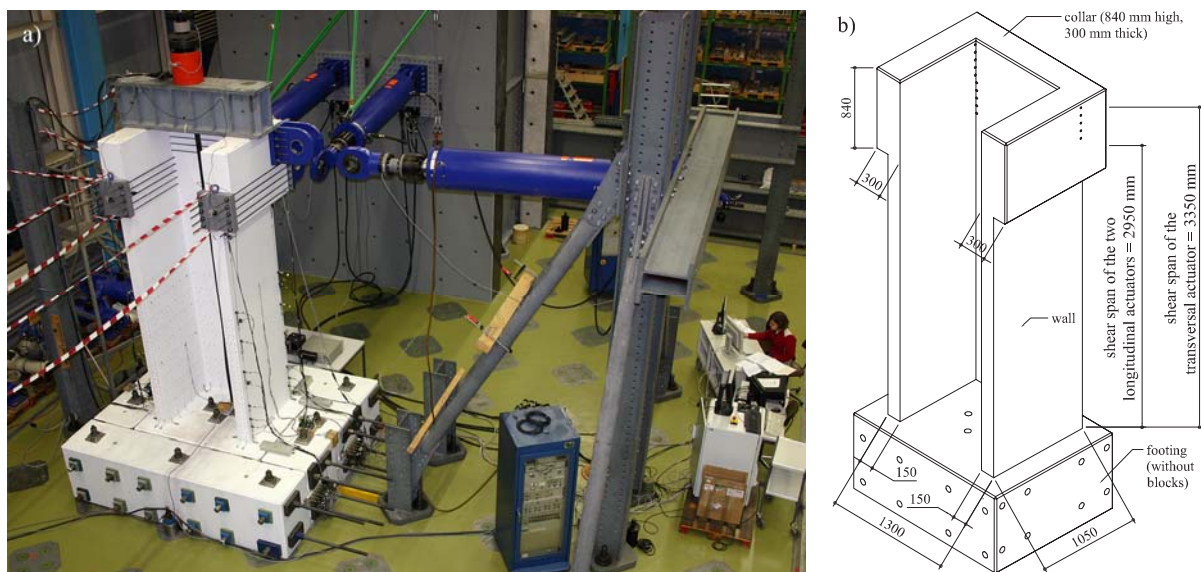


Figure 7: Test setup (a) and elevation of test unit A (b)

4.2 Loading History

The wall configuration tested at Ispra was built three times and each of the identical walls was tested with a different loading pattern. Wall 1 was solely loaded parallel to the flanges, Wall 2 only parallel to the web and Wall 3 was subjected to a rectangular clover leaf pattern [ECOEST2/ICONS, 2001]. This approach is possibly the ideal solution since all loading patterns are separated but it is very expensive. In the test program described here it had been decided to test two different wall configurations but to build each wall unit only once. The loading history had hence to be carefully considered since all essential loading directions and patterns had to be covered with one loading history. The chosen loading history is based on the pattern developed by Hines et al. [2002] who proposed a history comprising a “sweep” and a diagonal at each ductility level. The particularity of the “sweep” is that a yield displacement is also defined for the diagonal direction and hence the pattern seems to be more rounded than the rectangular clover leaf pattern which leads to larger displacements in the diagonal directions and tends to be too severe in the diagonal directions for the considered ductility level. In the tests described here, Hines’ et al. [2002] pattern is preceded by a full cycle parallel to the web and a full cycle parallel to the flanges. The complete loading history for one cycle is hence (see Figure 8a):

- Full cycle parallel to the web (O→A→B→O)
- Full cycle parallel to the flanges (O→C→D→O)
- Full cycle in diagonal direction (O→E→F→O)
- “Sweep” (O→A→G→D→C→H→B→O)

In addition to the cyclic displacements, small rotations at O, A, B, C and D are applied at ductility levels 1.0 and 4.0. Altogether, the load pattern is more severe than the load patterns used in Ispra or load patterns for uni-directional tests were the wall is typically subjected to two full cycles at the same ductility level. If the diagonal and the “sweep” are projected onto the principal directions the walls of this test program are subjected at each ductility level to three full cycles parallel to the web and to the flanges. The total loading history is the repetition of this load pattern at different ductility levels. The first four levels are within the elastic range of the wall. The amplitudes of these cycles are force-controlled with limits of 25%, 50%, 75% and 100% of the lateral forces at first yield according to the prediction. During these cycles the sweep was replaced by the second diagonal (O→G→H→O). After first yield of the reinforcement bars has been reached the nominal yield displacements in the five directions were determined on the basis of mean strains of vertical bars at the wall base in conjunction with the prediction made prior to the test. The loading pattern was repeated at displacement ductility levels of 1, 2, 3, 4, 6, 8 until failure occurred.

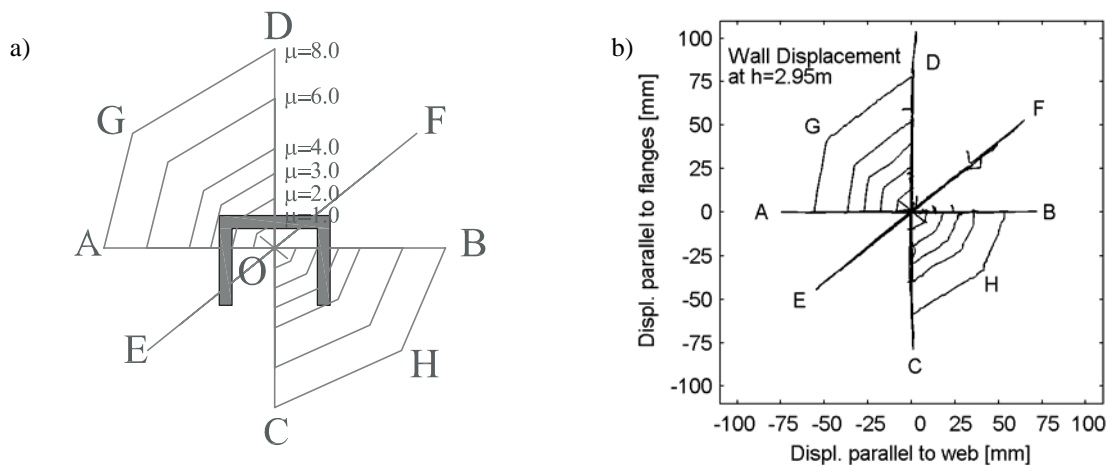


Figure 8: Displacement pattern: intended (a) and achieved (b)

5. PRELIMINARY RESULTS FOR TEST UNIT A

At the time of writing, the test of unit A was just completed. Preliminary results of this test are presented in the following. Figure 9 shows the force-displacement hystereses for the actuator acting parallel to the web and the actuators acting parallel to the flanges; for the latter the force of the two single actuators has been added together. Failure of the wall occurred at ductility 8 when the wall was loaded in the diagonal direction.

Significant spalling of the cover concrete had initiated during the cycles with ductility 4. In the following cycles spalling continued in particular at the extremities (flange ends and corners) but also at crossings of cracks. Crack widths were particularly large outside the boundary elements where low reinforcement ratios combined with the high concrete tensile strength lead to large distances between cracks. The test unit was able to complete the full loading pattern at ductility 6 reaching drifts of 1.9%, 2.0%, 2.6%, 1.8% and 2.1% at positions A, C, D, E and F respectively. Failure of the wall initiated during the first load steps of ductility 8. One or two D6 bars ruptured when loading during the cycle parallel to the web (A→B). During the load step parallel to the flanges from O→D the first D12 bar ruptured. When loading in the diagonal direction from E→F two further D12 bars and all remaining D6 bars in the flange under tension ruptured (Figure 10b). The D12 bars at the very flange end and some of the D6 bars had previously buckled in compression (Figure 10a) while one of the D12 bars and some D6 bars failed because their strain capacity had been reached. By this time the flange with the ruptured bars had lost most of its strength. Point 'F' at ductility 8 was therefore defined as the point of failure. At this stage sliding both parallel to flanges and web was still very minor.

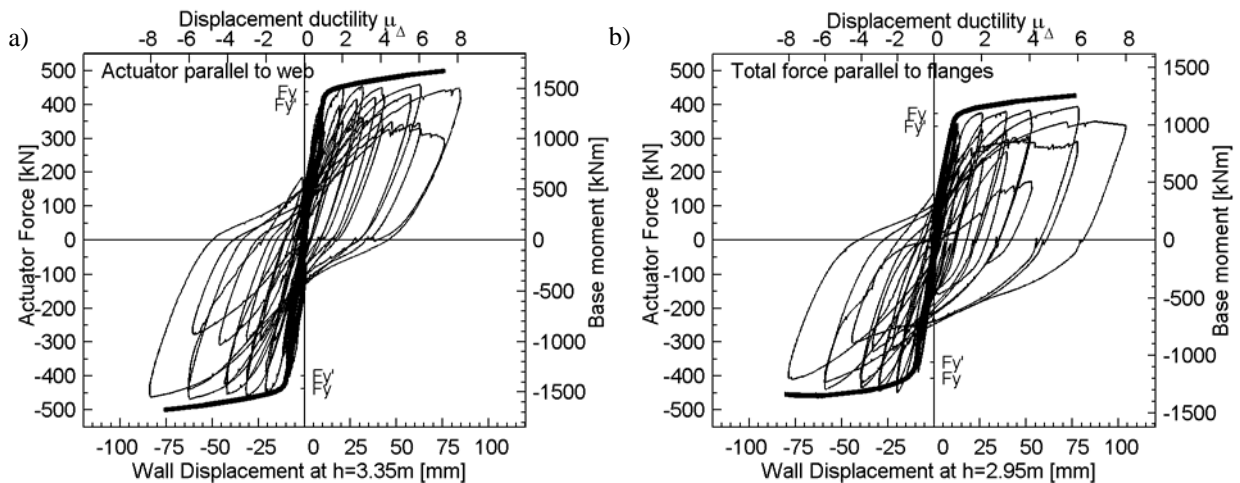


Figure 9: Test unit A: Force-displacement hysteresses for actuator parallel to web (a) and actuators parallel to flanges (b) including the predicted pushover-curves

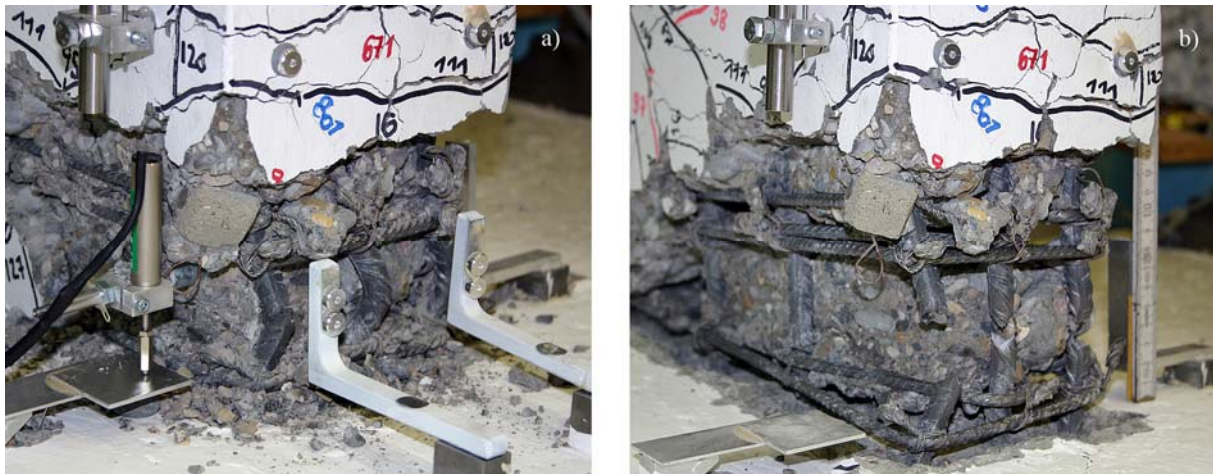


Figure 10: Test unit A: Photographs of flange end showing (a) one ruptured and the two buckled D12 bars ($\mu_d=8.0$, Point 'E') and (b) the three ruptured D12 bars ($\mu_d=8.0$, Point 'F')

6. SUMMARY

Compared to the number of experiments conducted in recent years on rectangular RC walls there is a general lack of experimental results for U-shaped walls under seismic loading. The aim of the presented study is to contribute to a better understanding of the latter by conducting quasi-static cyclic tests on two U-shaped walls with different wall thicknesses. This paper gives a brief summary of different aspects considered during the

planning stage of the experiments. This includes the steps required to reduce a U-shaped wall being part of a fictitious 6-storey reference building subjected to seismic loading to test units at 1:2 scale subjected to actuator forces at the wall heads. The main aspects considered in this process were the effective height at which the actuator forces were applied, the boundary condition at the wall head to torsion, the material properties and the loading history. Finally, prediction and preliminary results in the form of force-displacement hysteresis curves and a brief description of the failure mode of the first test unit were presented.

7. REFERENCES

- Dazio, A., Wenk, T. and Bachmann, H. (1999), Versuche an Stahlbetontragwänden unter zyklischer-statischer Einwirkung, *Technical Report, IBK Report Nr. 239*, Institute of Structural Engineering, Swiss Federal Institute of Technology, Zürich.
- Eurocode 8 (2003), Eurocode 8: Design provisions for earthquake resistance of structures, Part 1: General rules, seismic actions and rules for buildings, *Final Draft prEN 1998- 1*, European Committee for Standardization, Brussel, Belgium.
- ECOEST2/ICONS (2001), Shear walls, CAFEEL-ECOEST/ICONS Thematic report No. 5, 240 p., Editors: Reynouard, J.M. and Fardis, M.N., published by LNEC, Lisbon, Portugal.
- Elnashai, A., Pilakoutas, K. and Ambraseys, N. (1990), Experimental behaviour of reinforced concrete walls under earthquake loading, *Earthquake Engineering and Structural Dynamics*, 19, 389-407.
- Heidebrecht, A.C. and Stafford Smith, B. (1973), Approximative analysis of open-section shear walls subjected to torsional loading, *Journal of the Structural Division*, 2355-2373.
- Hines, E.M., Dazio, A., Chou, C.-C. and Seible, F., Structural Testing of the San Francisco-Oakland Bay Bridge East Span Skyway Piers, Report No. SSRP-2002/1, Department of Structural Engineering, University of California, San Diego, La Jolla, California, USA.
- Ile, N., Plumier, C. and Reynouard, J. (2002), Test program on U-shaped walls leading to model validation and implication to design, in *Proceedings of the 12th European Conference on Earthquake Engineering*, Elsevier Science Ltd.
- Ile, N. and Reynouard, J. (2005), Behaviour of U-shaped walls subjected to uniaxial and biaxial cyclic lateral loading, *Journal of Earthquake Engineering*, 9(1), 67-94.
- Kowalsky, M. and Priestley, M.J.N. (2000), Improved analytical model for shear strength of circular reinforced concrete columns in seismic regions, *ACI Structural Journal*, 97(3), 388-396.
- Lestuzzi, P., Wenk, T. and Bachmann, H. (1999), Dynamische Versuche an Stahlbetontragwänden auf dem ETH-Erdbebensimulator, *Technical Report, IBK Report Nr. 240*, Institute of Structural Engineering, Swiss Federal Institute of Technology, Zürich, Switzerland.
- Mazzoni, S., McKenna, F. and Fenves, G. L. (2005), OpenSees Command Language Manual for OpenSees v1.6; University of California, Berkeley, California, USA
- NZS3101 (2006), New Zealand Standard: Concrete Structures Standard – The Design of Concrete Structures, *Part 1 and Part 2 (Commentary)*, Standards New Zealand.
- Oesterle, R.G., Fiorato, A.E. and Corley, W.G. (1980), Reinforcement Details for Earthquake-Resistant Structural Walls, Research and Development Bulletin RD073.01D, Portland Cement Association.
- Paulay, T. and Priestley, M.J.N. (1992), Seismic Design of Reinforced Concrete and Masonry Buildings, *John Wiley & Sons*, New York, USA.
- Paulay, T., Priestley, M.J.N. and Syngge, A. (1982), Ductility in earthquake resisting squat shearwalls, *ACI Journal*, 257-269.
- Petersen, C. (1997), Stahlbau – Grundlagen der Berechnung und baulichen Ausbildung von Stahlbauten, 2nd print of 3rd edition, Vieweg, Braunschweig/Wiesbaden, Germany.
- Salonikis, T., Kappos, A., Tegos, I. and Penelis, G. (1999), Cyclic load behaviour of low-slenderness reinforced concrete walls: Failure modes, strength and deformation analysis, and design implications, *ACI Structural Journal*, 132-141.
- SIA262 (2004), Betonbau, Schweizer Norm SN 505 262, Schweizerischer Ingenieur- und Architekten-Verein, Zürich, Switzerland.
- Vallenas, J.M., Bertrero, V.V., Popov, E.P. (1979), Hysteretic Behavior of Reinforced Concrete Structural Walls, *Report UBC/EERC-79/20*, University of California, Berkeley, California, USA.